

Supplementary Information

Heterogeneous and self-organizing mineralization of bone matrix promoted by hydroxyapatite nanoparticles

G. Campi^{a,°}, F. Cristofaro^{b,c,°}, G. Pani^d, M. Fratini^{e,f}, B. Pascucci^a, P.A. Corsetto^d, B. Weinhausen^g, A. Cedola^e, A.M. Rizzo^{*d}, L. Visai^{*b,c}, G. Rea^{*a}

^a Institute of Crystallography - CNR, via Salaria Km 29.300, 00015, Monterotondo Roma, Italy

^b Molecular Medicine Department (DMM), Center for Health Technologies (CHT), UdR INSTM, University of Pavia, Viale Taramelli 3/B – 27100 Pavia – ITALY

^c Department of Occupational Medicine, Toxicology and Environmental Risks, Istituti Clinici Scientifici Maugeri S.p.A, IRCCS, Via S. Boezio, 28 - 27100 Pavia – ITALY

^d Department of Pharmacological and Biomolecular Sciences, Università degli Studi di Milano, via D. Trentacoste 2, 20134 Milano, Italy.

^e Institute of Nanotechnology-CNR c/o Physics Department at 'Sapienza' University, Piazzale Aldo Moro 2, 00185 Rome, Italy

^f Fondazione Santa Lucia I.R.C.C.S., Via Ardeatina 306, 00179 Roma, Italy

^g European Synchrotron Radiation Facility, B. P. 220, F-38043 Grenoble Cedex, France

[°] Both authors contributed equally to this article

*Corresponding authors:

giuseppina.rea@ic.cnr.it, livia.visai@unipv.it, angelamaria.rizzo@unimi.it

Figures and figure legends

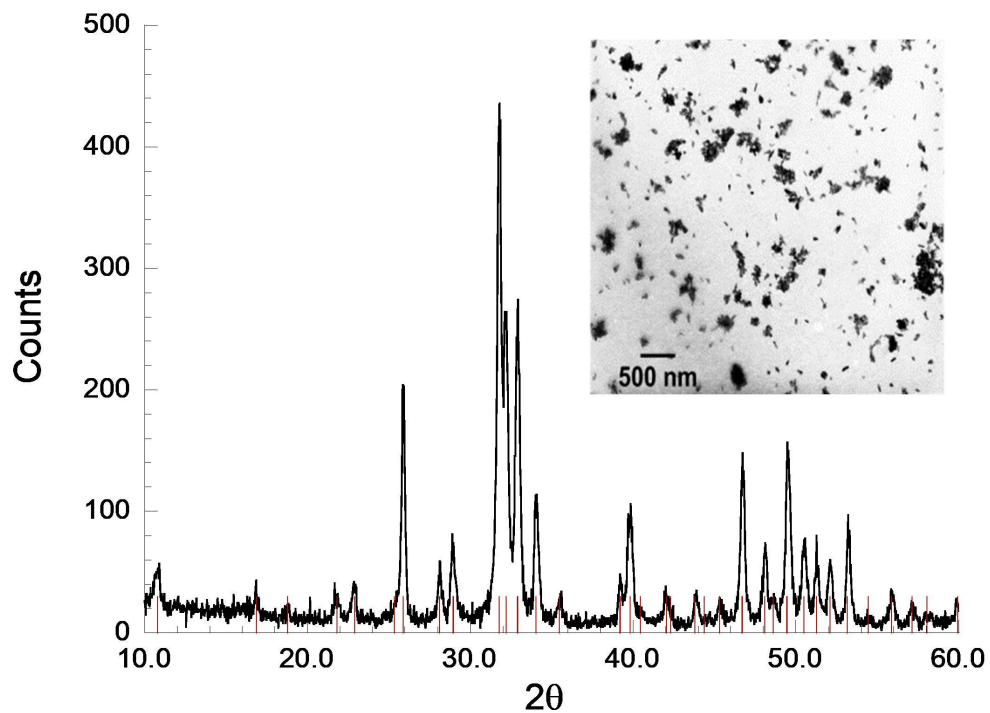


Fig. 1 SI: nHAP particles characterization

X Ray Diffraction pattern of externally supplied nHap particle indicating their polycrystalline nature; the red marker indicate the peak position of the $\text{Ca}_5(\text{PO}_4)_3(\text{OH})$ structure with P63/m symmetry. In the inset we show representative TEM images of nHap at 20.000X (A) magnification. Scale bars represent 500 nm.

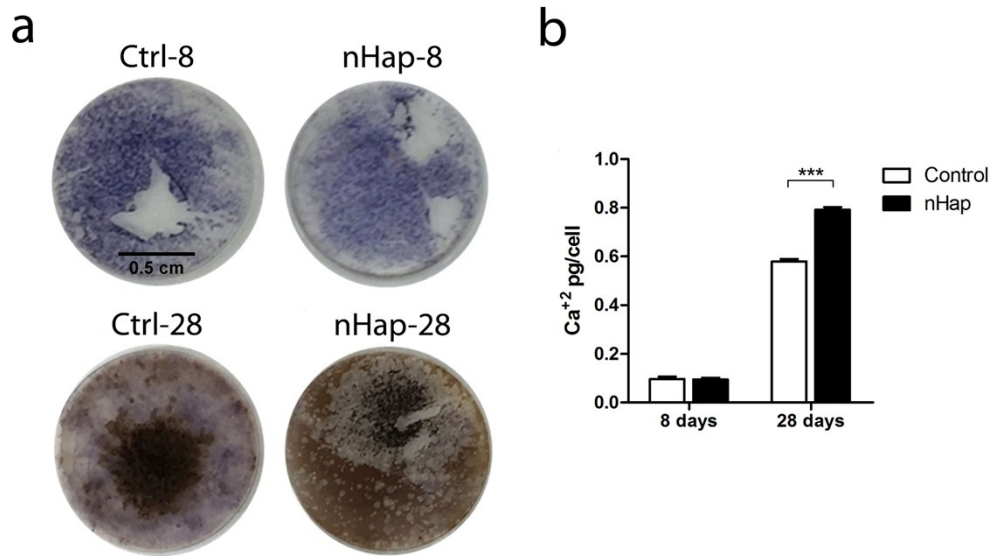


Figure 2 SI: Differentiation and bio-mineralization of hBM-MSCs. (a) Alkaline phosphatase (blue) and mineral deposition (black) staining of Ctrl-8, nHap-8, Ctrl-28 and nHap-28 samples of hBM-MSCs. (b) Quantitative evaluation of deposited Ca performed by Calcium–cresolphthalein complexone method as reported in material and methods section. Bars represent mean and SEM of three experiments. Statistical analysis was performed against control (**p<0,001; n=3).

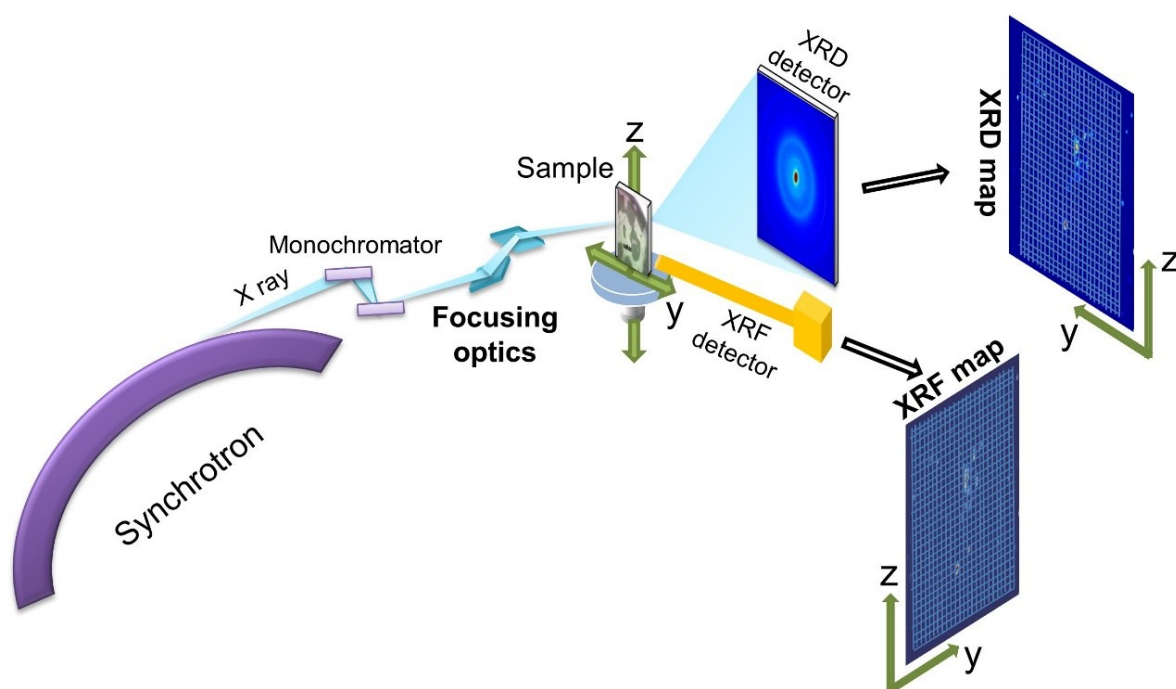


Figure 3 SI: Experimental setup for simultaneous Scanning X ray Diffraction and Fluorescence measurements.

Layout of experimental setup adopted for high-resolution synchrotron scanning X-ray micro-diffraction. The monochromatic X-ray beam is focused on a $2 \times 2 \mu\text{m}^2$ spot on the sample. A single X-ray diffraction frame and a single X ray fluorescence pattern are collected at each (y, z) position. In this way, we build maps of hydroxyapatite nanocrystals and Calcium by scanning the sample with a step of $2 \mu\text{m}$ in both horizontal and vertical direction.

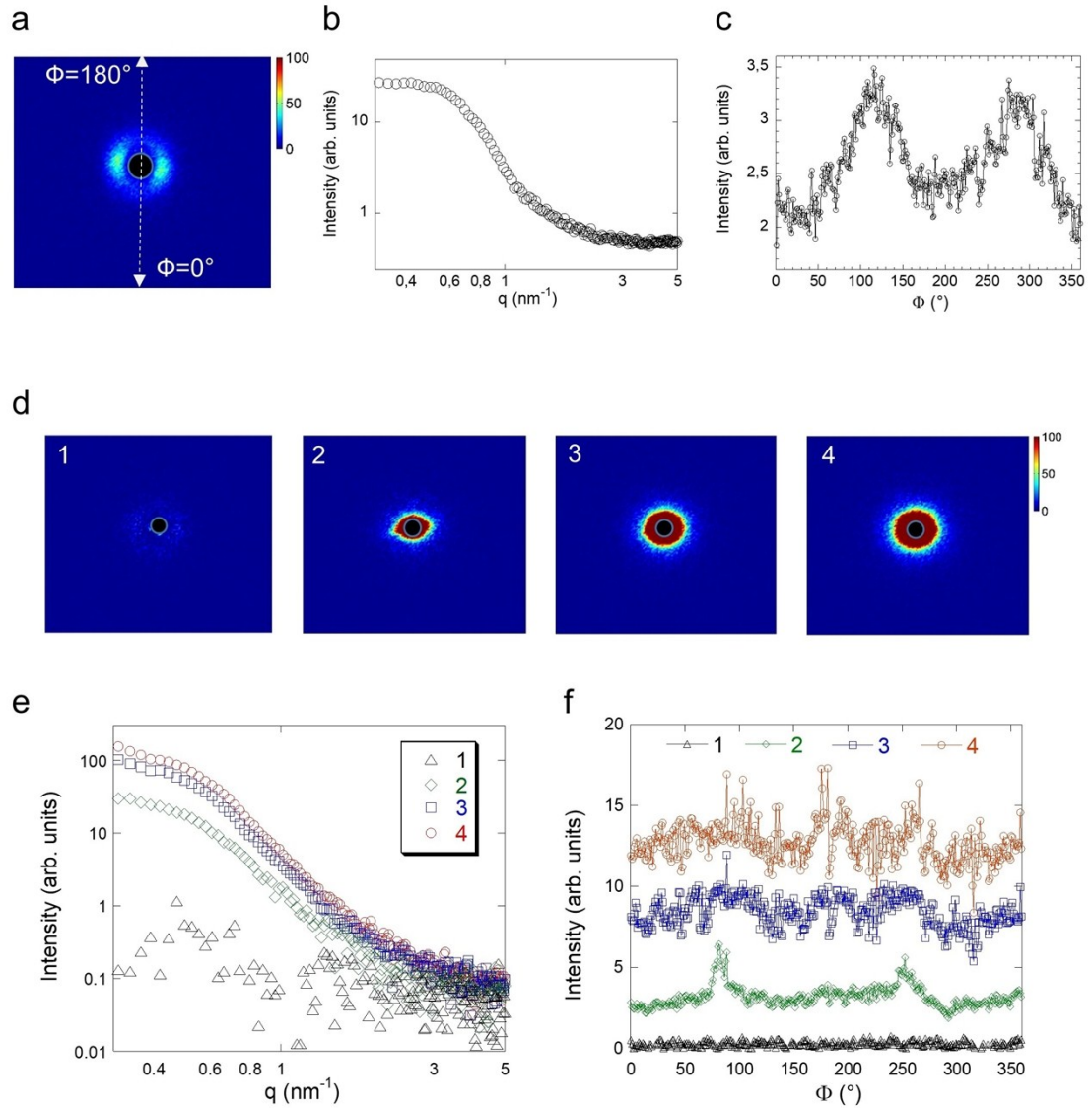


Figure 4 SI: 2D SAXS Frames and Background subtraction

(a) Typical 2D SAXS pattern of thermnox support showing the preferred orientations. (b) Radially and (c) azimuthally integrated SAXS profiles, $I(q)$ and $I(\Phi)$. We get the preferred orientations indicated by the two peaks at about 100° and 280° in $I(\Phi)$. (d) Typical 2D SAXS patterns with thermnox subtracted in four different points of a nhap-28 sample. SAXS profiles extracted from (e) radial and (f) azimuthal integration of 2D SAXS patterns 1, 2, 3 and 4 in (d) and normalized for the incident flux. In 1 we do not have any appreciable signal. The 2 indicates a poorly mineralized 2×2 area where we can observe preferred orientations consistent with the thermnox orientation. This orientation disappears as the mineralization increases, in 3 and 4.

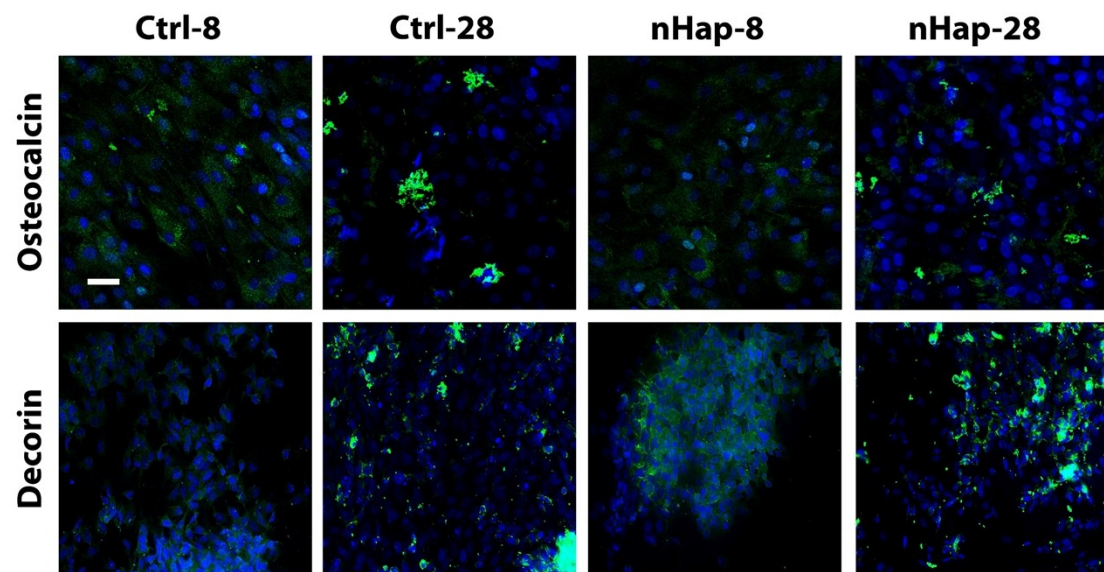


Figure 5 SI: deposition of extracellular matrix proteins during differentiation.

hBM-MSCs immunostaining of osteocalcin and decorin deposited in Ctrl-8, Ctrl-28, nHap-8 and nHap-28. hBMSCs were seeded and incubated without/with nHap suspension for 8 and 28 days, respectively. At the end of each incubation time, cells were fixed and immunostained against bone proteins as indicated in Materials and Methods section. Nuclei were counterstained with Hoechst 33342 (blue) and the extracellular deposits of bone proteins like osteocalcin and decorin were probed with a fluorescent secondary antibody (green). The bar corresponds to 50 μm.

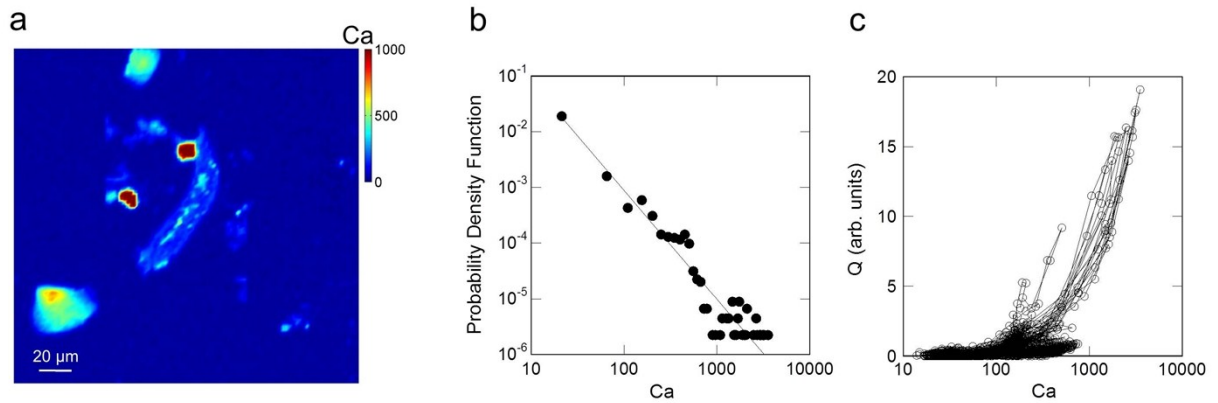


Figure 6 SI: Typical spatial distribution of Ca in differentiated human stem cells to osteoblasts.

(a) Map of the integrated area of the Ca peaks (shown in Figure 3c) indicating the Calcium content in the nHap-28 sample. The map appears quite similar to the Q map measured in the same sample ROI shown in Figure 4. Indeed, we find a high correlation coefficient between the Q and Ca maps, equal to 0.88 (b) Probability Density Function of the Calcium content, showing a power law behavior with exponent equal to 2.0 ± 0.6 . (c) Semilogarithmetic scatter plot of the Q intensity vs. Ca content, indicating the high correlation between the Q SAXS signal and the Ca content.

Tables

Table I SI: Primers used for qrtPCR.

Gene	Forward primer	Reverse primer
<i>ALP</i>	5'- ACCTCGTTGACACCTGGAAG - 3'	5'- CCACCATCTCGGAGAGTGAC - 3'
<i>IBSP</i>	5'- GGGCAGTAGTGACTCATCCG - 3'	5'- TCAGCCTCAGAGTCTTCATCTTC - 3'
<i>OCN</i>	5'- GGCAGCGAGGTAGTGAAGAG - 3'	5'- CTGGAGAGGAGCAGAACTGG - 3'
<i>DCN</i>	5'- CGAGTGGTCCAGTGTTCTGA - 3'	5'- AAAGCCCCATTTTCAATTCC - 3'
<i>18S</i>	5'- GTAACCCGTTGAACCCCAT - 3'	5'- CCATCCAATCGGTAGTAGCG - 3'